AMERICAN SOCIETY FOR MICROBIOLOGY | Journal of Virology®

GENOME REPLICATION AND REGULATION OF VIRAL GENE EXPRESSION

Experimental Analysis of Mimivirus Translation Initiation Factor 4a Reveals Its Importance in Viral Protein Translation during Infection of *Acanthamoeba polyphaga*

Meriem Bekliz,[a] Said Azza,[a] Hervé Seligmann,[a] Philippe Decloquement,[a] Didier Raoult,[a] Bernard La Scola[a]

[a]Unité de Recherche sur les Maladies Infectieuses et Tropicales Emergentes (URMITE), Aix-Marseille Université, UM63 IRD 198, IHU-Méditerranée Infection, Marseille, France

ABSTRACT The *Acanthamoeba polyphaga* mimivirus is the first giant virus ever described, with a 1.2-Mb genome which encodes 979 proteins, including central components of the translation apparatus. One of these proteins, R458, was predicted to initiate translation, although its specific role remains unknown. We silenced the R458 gene using small interfering RNA (siRNA) and compared levels of viral fitness and protein expression in silenced versus wild-type mimivirus. Silencing decreased the growth rate, but viral particle production at the end of the viral cycle was unaffected. A comparative proteomic approach using two-dimensional difference-in-gel electrophoresis (2D-DIGE) revealed deregulation of the expression of 32 proteins in silenced mimivirus, which were defined as up- or downregulated. Besides revealing proteins with unknown functions, silencing R458 also revealed deregulation in proteins associated with viral particle structures, transcriptional machinery, oxidative pathways, modification of proteins/lipids, and DNA topology/repair. Most of these proteins belong to genes transcribed at the end of the viral cycle. Overall, our data suggest that the R458 protein regulates the expression of mimivirus proteins and, thus, that mimivirus translational proteins may not be strictly redundant in relation to those from the amoeba host. As is the case for eukaryotic initiation factor 4a (eIF4a), the R458 protein is the prototypical member of the ATP-dependent DEAD box RNA helicase mechanism. We suggest that the R458 protein is required to unwind the secondary structures at the 5′ ends of mRNAs and to bind the mRNA to the ribosome, making it possible to scan for the start codon. These data are the first experimental evidence of mimivirus translation-related genes, predicted to initiate protein biosynthesis.

IMPORTANCE The presence in the genome of a mimivirus of genes coding for many translational processes, with the exception of ribosome constituents, has been the subject of debate since its discovery in 2003. In this work, we focused on the R458 mimivirus gene, predicted to initiate protein biosynthesis. After silencing was performed, we observed that it has no major effect on mimivirus multiplication but that it affects protein expression and fitness. This suggests that it is effectively used by mimivirus during its developmental cycle. Until large-scale genetic manipulation of giant viruses becomes possible, the silencing strategy used here on mimivirus translation-related factors will open the way to understanding the functions of these translational genes.

KEYWORDS mimivirus, R458, translation, protein expression, gene silencing, giant virus

The *Acanthamoeba polyphaga* mimivirus is the first giant virus to have been described in terms of both particle size and genome complexity (1). It is representative of an expanding family of giant viruses infecting *Acanthamoeba* (2). Together with

Received 28 February 2018 **Accepted** 28 February 2018

Accepted manuscript posted online 7 March 2018

Citation Bekliz M, Azza S, Seligmann H, Decloquement P, Raoult D, La Scola B. 2018. Experimental analysis of mimivirus translation initiation factor 4a reveals its importance in viral protein translation during infection of *Acanthamoeba polyphaga*. J Virol 92:e00337-18. https://doi.org/10.1128/JVI.00337-18.

Editor Rozanne M. Sandri-Goldin, University of California, Irvine

Copyright © 2018 American Society for Microbiology. All Rights Reserved.

Address correspondence to Bernard La Scola, bernard.la-scola@univ-amu.fr.

TABLE 1 Mimivirus translation-related gene products

Mimivirus category	Translation-related gene product(s)	Function(s)	ORF(s)
Aminoacyl-tRNA synthetases (aa-RSs)	Arginyl-RS (Arg-RS)	Acting as genuine enzymes	R663
	Cysteinyl-RS (Cys-RS)		L164
	Methionyl-RS (Met-RS)		R639
	Tyrosyl-RS (Tyr-RS)		L124
tRNAs	Leucine (3×)	TAA, TAA, and TTG	L46, R875, R902
	Histidine	CAC	MIMI_gt0002
	Cysteine	TGC	L276
	Tryptophan	TGG	R868
Translation-related factors	IF4A	Initiation factor	R458
	IF4E	Initiation factor	L496
	SUI1	Initiation factor	R464
	eF-TU	Elongation factor	R624
	eRF1	Termination factor	R726

other families of giant viruses, it composes a new proposed order called *Megavirales* (2). The original features of mimivirus are its unexpectedly large diameter, encapsulating a 1.2-Mb double-stranded DNA genome, and the nature of the genes carried by it (3). The mimivirus genome includes an arsenal of genes, among which more than 70% of the predicted genes either are open reading frame orphan genes (ORFans) or have unknown functions (3, 4). Furthermore, the most emblematic and impressive of the mimivirus genes are those that encode functions which have never been encountered in any virus as translation components, triggering considerable interest in evolutionary biology (5–7). The mimivirus prototype is predicted to encode five central translation-related factors. Three of the factors encode proteins involved in translation initiation, the most important step in translation, and the other two factors are involved in peptide elongation and translation termination (7, 8) (Table 1). In addition, mimivirus encode four aminoacyl-tRNA synthetases (aa-RSs) and six tRNAs (3) (Table 1). These aa-RSs and tRNAs link the genetic code to some of the 20 amino acids and are key molecules of basic translation genes (8). Moreover, the set of tRNAs and aa-RSs in mimivirus clearly differs from their known host cellular counterparts, which excludes the possibility that they originate from simple horizontal gene transfer (9, 10). The large arsenal of mimivirus genes, and particularly, the presence of genes related to translation, suggests that mimivirus is relatively independent of its host organism with regard to multiplication and mRNA translation. However, mimivirus remains dependent on the synthesis machinery of its amoeba host to translate its own proteins, due to its lack of ribosomes.

Until now, to the best of our knowledge, there have been no experimental studies of the function of mimivirus translation-related factors. Here, we used RNA silencing (small interfering RNA [siRNA]) (11) to repress the expression of one mimivirus translational gene to identify its possible involvement in translation. We focused on the gene encoding protein R458, which is predicted to be implicated in the initiation of translation. R458 exhibits a temporal expression pattern starting 3 h (H3) postinfection, just after the eclipse phase, which indicates the beginning of translation and protein synthesis (4). This protein appears to have originated from multiple eukaryotic initiation factor 4a (eIF4a), which is an abundant cytoplasmic protein (12–14). It is required to unwind any hairpin loops in the mRNA and to bind mRNAs to the ribosomal subunits in order to guarantee the start codon (AUG). This suggests that the R458 protein may play a major role in the initiation of translation in mimivirus (10). Here, we investigated whether mimivirus uses an alternative system of protein translation in relation to this protein R458, independently of that of its host. For this purpose, we compared the protein expression profiles and levels of virus fitness of a wild-type mimivirus and a silenced mimivirus.

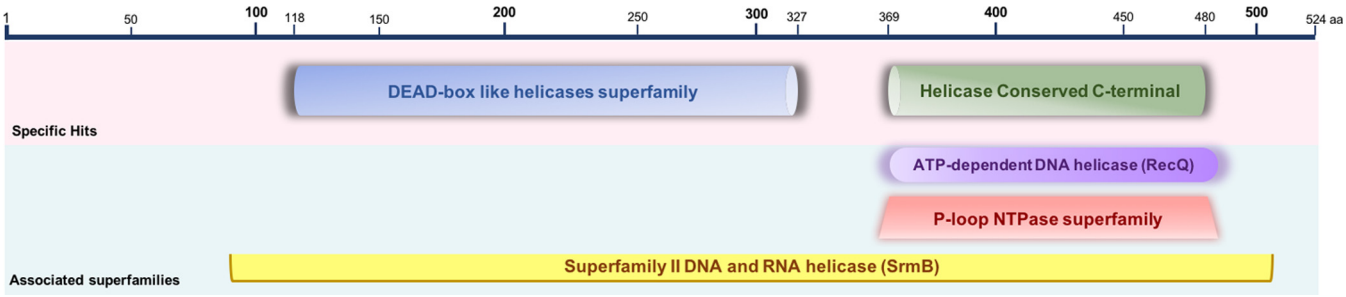

FIG 1 A schematic representation of putative conserved domains in R458 protein. Prediction of putative conserved domains in R458 protein was performed by analysis of proteins using BLASTp search, Pfam, SMART, Phyre2, and CDD search database analyses. These analyses indicated the location nomenclature of five domains of sequence homology: the DEAD box-like helicase superfamily, superfamily II DNA and RNA helicase (SrmB), helicase conserved C terminus, ATP-dependent DNA helicase (RecQ), and P-loop NTPase superfamily.

RESULTS

Bioinformatic analyses. We analyzed the genomic conserved domains of the R458 protein for the presence of putative conserved domains and related motifs, as identified in eIF4a, its homologue in eukaryotes. We found that this protein carries the conserved domains for members of the DEAD box-like helicase superfamily; helicase conserved c-terminal, associated with a putative superfamily II DNA and RNA helicase (SrmB); ATP-dependent DNA helicase (RecQ); and members of the P-loop NTPase superfamily (p loop containing nucleoside triphosphate hydrolases) (Fig. 1). On the basis of structural similarity searches, this protein has been modeled as a Bloom's syndrome helicase protein (100% identity), a member of the RecQ family of DNA helicases, which play key roles in maintaining genome integrity in all organism groups, especially in eukaryotes (15). The R458 protein contains domains and motifs that are characteristic of the eukaryotic translational initiation factor eIF4a. In summary, genomic analyses revealed that the R458 protein contains several conserved domains reminiscent of those associated with the eIF4a protein in eukaryotes. This protein could, therefore, play a major role in initiation of translation in mimivirus.

Studying the multiplication and fitness of mimivirus with and without R458. (i) Efficiency of R458 silencing. One duplex of siRNA was used to repress expression of the R458 transcript in mimivirus. In this experiment, fluorescent R458-siRNA was transfected in *A. polyphaga* infected by mimivirus using Lipofectamine. At 3 h postinfection, fluorescence was detected inside the amoeba, thus confirming transfection (Fig. 2). At 6 h postinfection, mimivirus RNA was extracted. Primers were designed to detect mRNA levels of R458 in both wild-type and silenced mimivirus using reverse transcription-PCR (RT-PCR). As indicated in Fig. 3, successful silencing of R458 was observed using the siRNA duplex. The mRNA expression level of R458 decreased significantly in response to treatment with R458-siRNA compared to the wild-type mimivirus. This confirmed that use of the siRNA designed for the R458 gene is a fast and effective method of reducing R458 expression levels in mimivirus.

(ii) Effect of silencing of R458 on DNA mimivirus replication and multiplication of mimivirus particles. To understand the effect of the absence of the R458 protein on translation, we studied the replication of mimivirus in the presence and in the absence of R458. The replication was examined in both wild-type and silenced mimivirus, searching for any abnormal features in its development. No significant differences in DNA replication were observed between wild-type and silenced mimivirus in different samples taken at 0, 8, 16, and 24 h postinfection (Fig. 4). In addition, using endpoint dilution assay, we did not observe a difference in mimivirus multiplication results between wild-type and silenced mimivirus in different samples taken at 0, 8, 16, and 24 h postinfection (Fig. 5). In addition, the growth monitoring of the second-generation DNA mimivirus showed no significant differences in replication between the descendants of wild-type and silenced mimivirus.

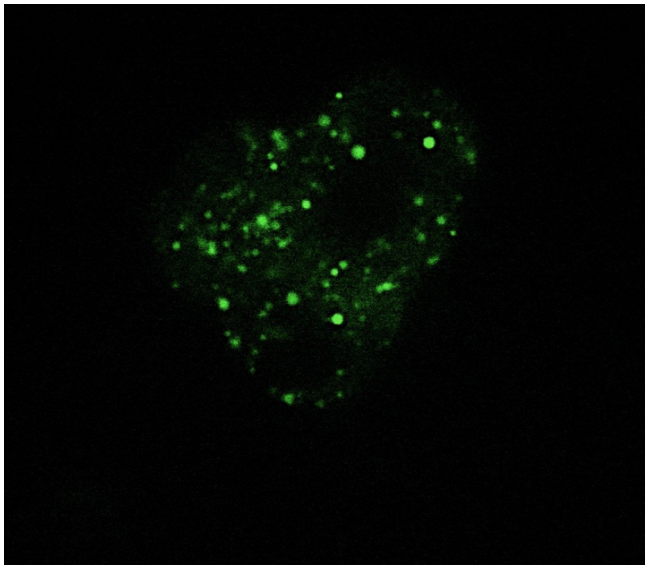

FIG 2 Control of siRNA transfection in amoeba revealed by visualization of the green fluorescence of oligonucleotides. The siRNA fluorescence was checked at 3 h postinfection as a control for a good transfection.

Thus, silencing of R458 did not significantly affect mimivirus multiplication. (All values presented in Fig. 4 and 5 represent means of results from three independent experiments.)

(iii) Effects of silencing of R458 on mimivirus fitness. We then followed the development cycle of wild-type and silenced mimivirus using immunodetection by fluorescence microscopy and mimivirus-specific polyclonal antibodies to observe the effects of R458 silencing on mimivirus growth. We observed that the eclipse-phase step was significantly longer in silenced mimivirus than in wild-type mimivirus (Fig. 6). The wild-type mimivirus entered the eclipse phase between H4 and H7 postinfection, while the silenced mimivirus entered the eclipse phase from H9 postinfection. Thus, there was a difference in the first appearance of virus factories, which was delayed by at least 2 h in silenced mimivirus compared to wild-type mimivirus.

In addition, immunodetection was also used to quantify numbers of virus factories in wild-type and silenced mimivirus at 7, 9, and 12 h postinfection. The numbers of virus

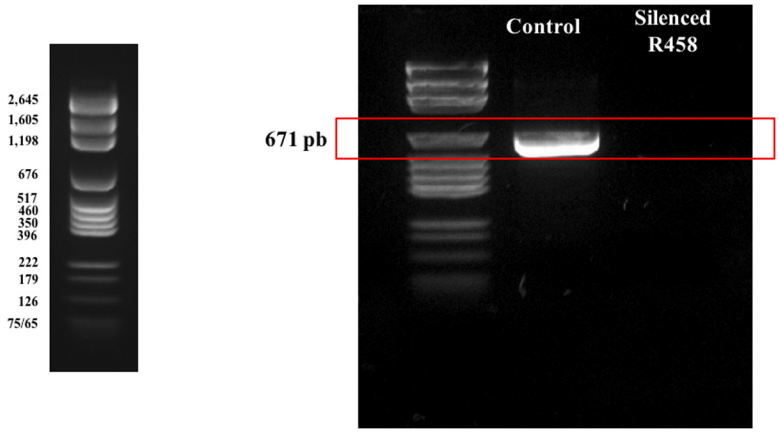

FIG 3 Downregulation of R458 in mimivirus using specific siRNA and RT-PCR analysis. Agarose gel electrophoresis showed the siRNA effect on R458 expression. RT-PCR analysis was done with total RNA extracted from wild-type mimivirus and siRNA-transfected mimivirus, showing R458 downregulation at the mRNA level. Amplification of R458 was done using specific primers listed in Table 4. pb, base pairs.

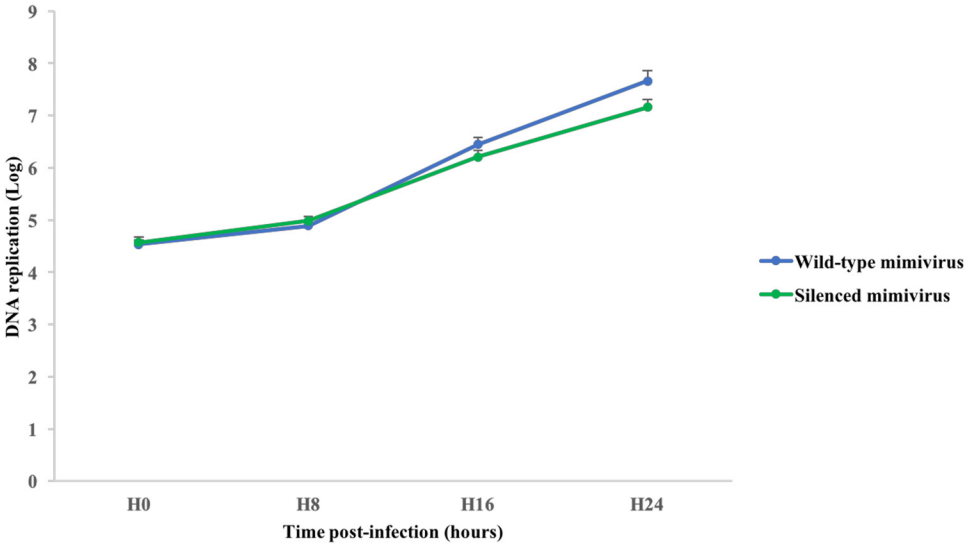

FIG 4 Kinetics of mimivirus DNA replication in both wild-type and silenced mimivirus. Growth analysis of wild-type mimivirus and silenced mimivirus in amoeba-infected cells by qPCR at 0, 8, 16, and 24 h postinfection at an MOI of 0.2. The *x* axis shows the time points, and the *y* axis shows the log concentration of mimivirus DNA (all values represent means of results from three independent assays).

factories in both wild-type and silenced mimivirus were estimated by random selection of 1,000 infected amoeba cells. The quantification revealed significant differences between wild-type and silenced mimivirus in the numbers of virus factories observed for each selected time point (Fig. 7). At 7 h postinfection, the numbers of mimivirus factories were around 10 and 0 factories per 1,000 infected amoeba cells in wild-type and silenced mimivirus, respectively. At 9 h postinfection, numbers of virus factories were about 43 and 15 factories per 1,000 infected amoeba cells in wild-type and silenced mimivirus, respectively. At 12 h postinfection, the numbers of virus factories were about 71 and 29 factories per 1,000 infected amoeba cells in wild-type and silenced mimivirus, respectively. The numbers of amoebas infected with silenced or wild-type mimivirus increased progressively until total cell lysis at 24 h postinfection without changing the final concentration of mimivirus particles in either wild-type or

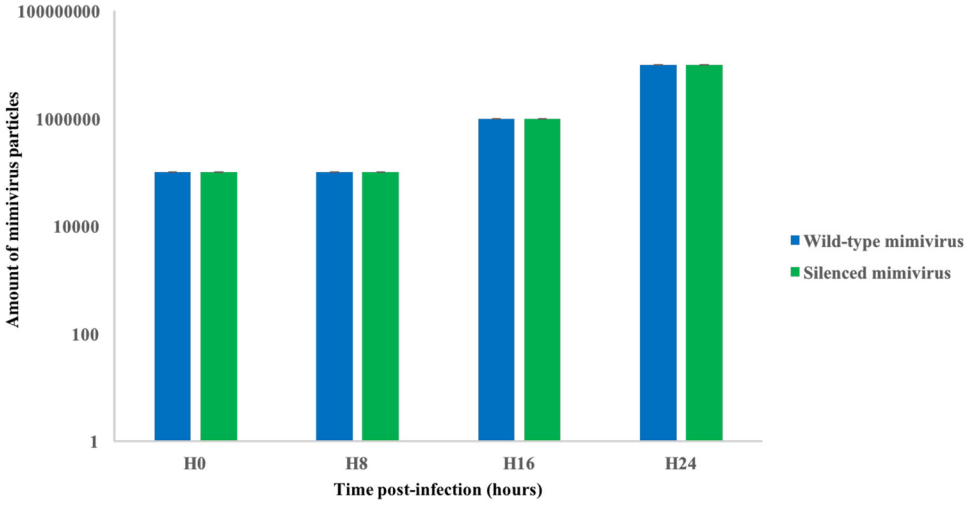

FIG 5 Analysis of mimivirus particle accumulation based on endpoint dilution assays demonstrating an evaluation of mimivirus multiplication. Titers were determined from supernatants of amoeba cells infected with wild-type mimivirus and silenced mimivirus at the designated time points (h 0 [H0], H8, H16, and H24) in triplicate. The *x* axis shows the time points, and the *y* axis shows the mimivirus particle accumulation.

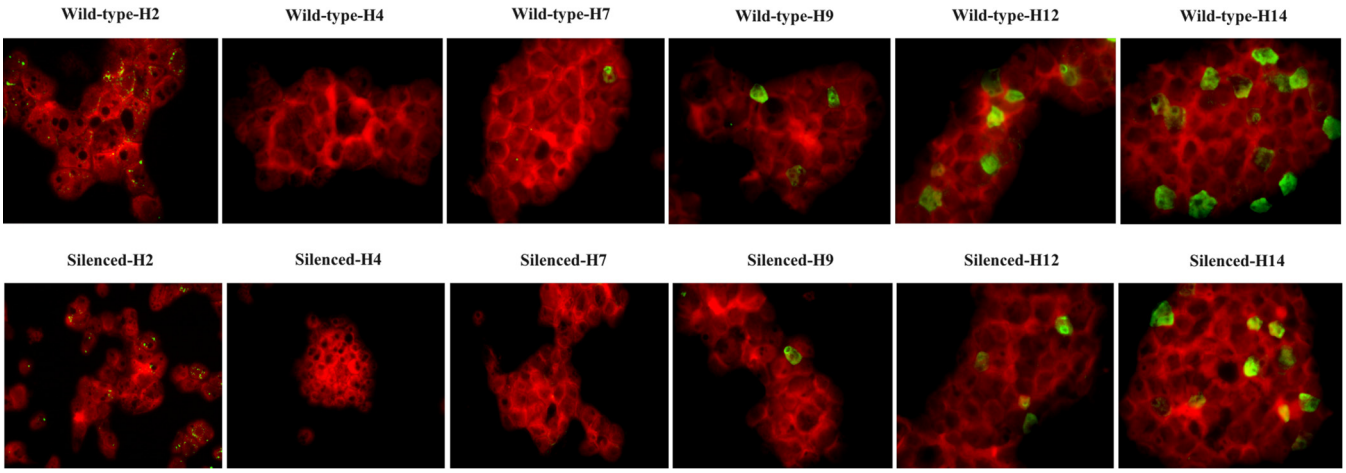

FIG 6 The development cycles of wild-type and silenced mimivirus. The cycles were demonstrated using fluorescence microscopy and mimivirus-specific polyclonal antibodies in three replicates. At H4, during the eclipse phase, mimivirus was not detected in either wild-type or silenced mimivirus. At H7, perinuclear particles become visible only in wild-type mimivirus. At H9, the first appearance of perinuclear particles in silenced mimivirus occurred. At H14, the number of amoebae infected with mimivirus particles was found to have increased progressively.

silenced mimivirus. All reported observations correspond to what was observed in 3 independent essays. To conclude, immunodetection with mimivirus-specific polyclonal antibodies made it possible to detect the delayed growth of mimivirus after silencing for R458 protein expression, although quantitative PCR (qPCR) showed no change in final numbers of produced viral particles.

The study of mimivirus protein expression: comparative proteomics study of wild-type and silenced mimivirus. To evaluate the effect of the R458 gene on protein expression, wild-type mimivirus and mimivirus silenced for this gene were collected, processed, and subjected to comparative proteomic analysis using two-dimensional difference-in-gel electrophoresis (2D-DIGE), as previously described (16). To assess changes in the protein profiles of wild-type and silenced mimivirus, four 2D-DIGE gels

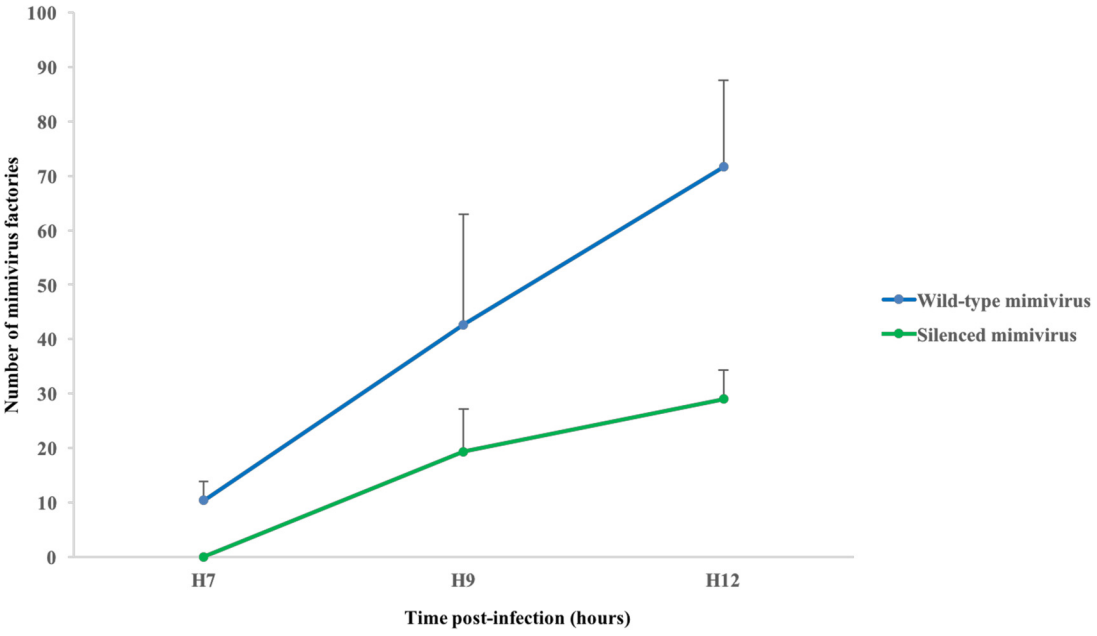

FIG 7 Quantification of virus factories in both wild-type and silenced mimivirus by randomly selecting 1,000 infected amoeba cells using the immunodetection method. The *x* axis shows the time points, and the *y* axis shows the mimivirus factory numbers (all values represent means of results from three replicates).

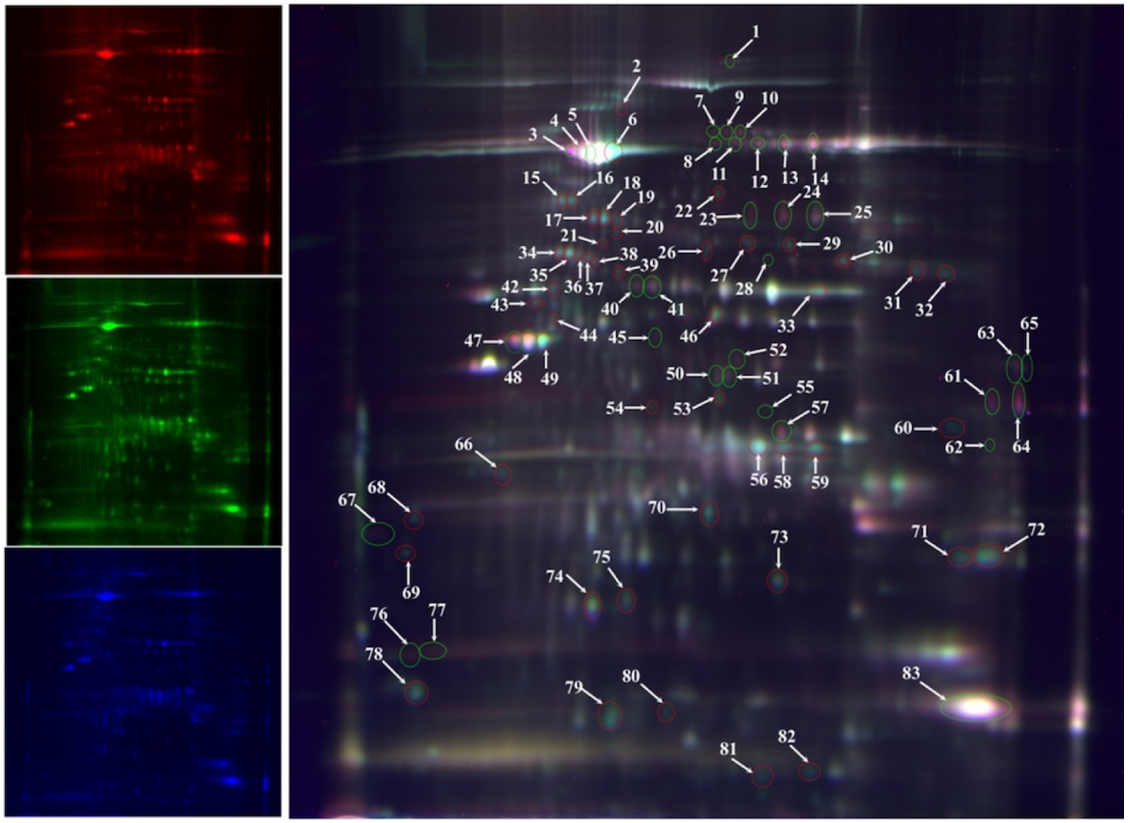

FIG 8 Representative 2D differential gel electrophoresis (2D-DIGE) analysis for comparative expression proteomics in wild-type and silenced mimivirus. Each individual sample from wild-type and silenced mimivirus and a pooled reference sample were labeled using fluorescent dyes (Cy5, Cy3, and Cy2) and were then separated on the same gel using the 2D-DIGE system. Three images were obtained from each gel, and an overlay of the dye scan images was also obtained. Each scanned fluorescent image was analyzed using SameSpot analysis software. Selected protein spots exhibiting an ANOVA score lower than or close to 0.05 and a fold change value of at least 1.5 are indicated by circles and spot numbers as listed in Table 2.

were utilized (Fig. 8) and proteins were identified by matrix-assisted laser desorption ionization–time of flight mass spectrometry (MALDI-TOF MS) and/or nano-liquid chromatography MS (nano-LC-MS). The results obtained using these approaches revealed 83 deregulated peptide spots, 48 of which were identified as downregulated and 35 as upregulated (Table 2). Of the 83 deregulated peptide spots, 81 were successfully identified as corresponding to 32 different proteins, most of which were not resolved into single peptide spots (Table 2). Identified proteins are listed in Table 2 together with their predicted functions and are classified into broad functional categories.

(i) Downregulated spots. Of the 48 downregulated peptide spots, we found 20 proteins which presented confident MALDI-TOF matching scores (Table 2). The function was unknown for 13 of them (R161, L324, L330, L442, L452, R459, L612, R646, R648, L690, L725, L823, and L829), including 5 ORFan proteins (L330, L442, L452, R646, and L725). In addition, two proteins were found to be involved in the structure of viral particles (L410 and L425), three in oxidative pathways (R443, R584, and L498), one in transcription (L235), and one in DNA topology and repair (R345).

(ii) Upregulated spots. The upregulated peptide spots included 17 proteins identified with confident mass spectrum matching scores (Table 2). Eight of them (L442, R463, R513b, R553, L567, L591, L724, and L725), including five ORFan proteins (L442, R463, L591, L724, and L725), are of unknown function. In addition, two proteins are involved in the structure of viral particles (L410 and L425), two in transcription (L107 and R470), three in oxidative pathways (R135, R362, and R596), one in topology and DNA repair (R345), and one in modification of proteins and lipid (R526).

TABLE 2 Differentially expressed proteins

Regulation	Spot no.	ANOVA (*P*)	Fold change from wild type/silenced	Highest mean	Protein	Locus tag	Accession no.	Functional category[a]	Identification method
Down	2	8.56E−05	2.3	Wild type	Uncharacterized protein	R345	YP_003986848	DNA topology and repair	MALDI-MS
	6	2.02E−07	3	Wild type	Capsid protein	L425	YP_003986929	Particle structure	MALDI-MS
	15	3.52E−05	2.1	Wild type	Capsid protein	L425	YP_003986929	Particle structure	MALDI-MS
	16	4.35E−06	3.1	Wild type	Capsid protein	L425	YP_003986929	Particle structure	MALDI-MS
	17	0.00057	1.8	Wild type	Uncharacterized protein	L829	YP_003987362	Other	MALDI-MS
	18	7.55E−06	2.9	Wild type	Capsid protein	L425	YP_003986929	Particle structure	MALDI-MS
	19	5.54E−05	1.9	Wild type	Uncharacterized protein	L829	YP_003987362	Other	MALDI-MS
	20	0.00061	2.1	Wild type	Uncharacterized protein	L829	YP_003987362	Other	MALDI-MS
	21	7.28E−05	1.7	Wild type	Capsid protein	L425	YP_003986929	Particle structure	MALDI-MS
	22	0.00364	1.7	Wild type	Putative core protein	L410	YP_003986914	Particle structure	MALDI-MS
	26	9.15E−06	1.6	Wild type	Uncharacterized protein	L829	YP_003987362	Other	MALDI-MS
	27	0.00073	1.6	Wild type	Uncharacterized protein	R161	YP_003986653	Other	MALDI-MS
	29	6.85E−05	2.5	Wild type	Putative core protein	L410	YP_003986914	Particle structure	MALDI-MS
	30	0.03087	1.6	Wild type	Putative core protein	L410	YP_003986914	Particle structure	MALDI-MS
	31	0.00043	1.5	Wild type	Probable zinc-type alcohol dehydrogenase-like protein	L498	YP_003987010	Oxidative pathways	MALDI-MS
	32	2.33E−06	2.3	Wild type	Probable zinc-type alcohol dehydrogenase-like protein	L498	YP_003987010	Oxidative pathways	MALDI-MS
	33	0.00021	1.8	Wild type	Uncharacterized protein	L442	YP_003986949	ORFan	MALDI-MS
	34	0.00457	1.6	Wild type	Capsid protein	L425	YP_003986929	Particle structure	MALDI-MS
	35	0.00054	2	Wild type	Capsid protein	L425	YP_003986929	Particle structure	MALDI-MS
	36	7.00E−05	2	Wild type	Capsid protein	L425	YP_003986929	Particle structure	MALDI-MS
	37	1.42E−05	2.3	Wild type	Capsid protein	L425	YP_003986929	Particle structure	MALDI-MS
	38	1.98E−05	2	Wild type	Capsid protein	L425	YP_003986929	Particle structure	MALDI-MS
	39	0.00037	1.6	Wild type	Uncharacterized protein	L442	YP_003986949	ORFan	MALDI-MS
	42	0.00046	1.5	Wild type	Uncharacterized protein	L442	YP_003986949	ORFan	MALDI-MS
	43	0.00353	1.5	Wild type	Uncharacterized protein	R648	YP_003987168	Other	Nano-LC-MS
	44	0.00010	1.7	Wild type	Uncharacterized protein	L690	YP_003987217	Other	MALDI-MS
	46	0.00753	1.5	Wild type	Uncharacterized protein	L442	YP_003986949	ORFan	MALDI-MS
	49	4.62E−06	2.6	Wild type	Uncharacterized protein	L442	YP_003986949	ORFan	MALDI-MS
	53	3.06E−05	4.2	Wild type	Uncharacterized protein	L442	YP_003986949	ORFan	MALDI-MS
	54	0.00012	5.4	Wild type	Uncharacterized protein	L725	YP_003987254	ORFan	Nano-LC-MS
	56	1.04E−05	1.7	Wild type	Uncharacterized protein	L725	YP_003987254	ORFan	MALDI-MS
	58	3.61E−05	1.8	Wild type	Uncharacterized protein	L725	YP_003987254	ORFan	MALDI-MS
	59	5.04E−05	1.9	Wild type	Uncharacterized protein	L725	YP_003987254	ORFan	MALDI-MS
	60	3.35E−06	3.4	Wild type	Uncharacterized protein	R646	YP_003987166	ORFan	Nano-LC-MS
	66	0.00811	1.6	Wild type	Uncharacterized protein	L452	YP_003986959	ORFan	Nano-LC-MS
	68	2.29E−05	2.7	Wild type	Uncharacterized protein	L442	YP_003986949	ORFan	Nano-LC-MS
	69	3.48E−05	2.2	Wild type	Uncharacterized protein	L442	YP_003986949	ORFan	Nano-LC-MS
	70	6.68E−05	1.8	Wild type	Uncharacterized protein	L823	YP_003987355	Other	Nano-LC-MS
	71	0.00092	2.1	Wild type	Uncharacterized protein	R459	YP_003986856	ORFan	MALDI-MS
	72	5.14E−05	1.6	Wild type	DNA-directed RNA polymerase subunit 5	L235	YP_003986731	Transcription	MALDI-MS
	73	0.00423	1.5	Wild type	Uncharacterized N-acetyltransferase	R584	YP_003987099	Oxidative pathways	MALDI-MS
	74	0.00838	1.5	Wild type	Uncharacterized protein	L324	YP_003986827	Other	Nano-LC-MS
	75	0.00353	2.2	Wild type	Uncharacterized protein	L330	YP_003986833	ORFan	MALDI-MS
	78	0.00203	2.1	Wild type	Uncharacterized protein	L442	YP_003986949	ORFan	Nano-LC-MS
	79	1.98E−05	2.9	Wild type	Capsid protein	L425	YP_003986929	Particle structure	MALDI-MS
	80	0.00492	2	Wild type	Thioredoxin domain	R443	YP_003986950	Oxidative pathways	Nano-LC-MS
	81	0.00032	2.1	Wild type	Capsid protein	L425	YP_003986929	Particle structure	MALDI-MS
	82	0.00887	1.8	Wild type	Mannose-6P isomerase	L612	YP_003987129	Other	Nano-LC-MS
Up	1	2.62E−05	1.5	Silenced	Uncharacterized protein	R345	YP_003986848	DNA topology and repair	MALDI-MS
	3	3.93E−07	3.2	Silenced	Capsid protein	L425	YP_003986929	Particle structure	MALDI-MS
	4	1.71E−07	2.7	Silenced	Capsid protein	L425	YP_003986929	Particle structure	MALDI-MS
	5	2.06E−05	1.6	Silenced	Capsid protein	L425	YP_003986929	Particle structure	MALDI-MS
	7	3.10E−05	2.2	Silenced	Putative GMC-type oxidoreductase	R135	YP_003986627	Oxidative pathways	MALDI-MS
	8	3.88E−06	2.4	Silenced	Putative GMC-type oxidoreductase	R135	YP_003986627	Oxidative pathways	MALDI-MS
	9	3.26E−07	2.4	Silenced	Putative GMC-type oxidoreductase	R135	YP_003986627	Oxidative pathways	MALDI-MS
	10	1.13E−05	1.8	Silenced	Putative GMC-type oxidoreductase	R135	YP_003986627	Oxidative pathways	MALDI-MS
	11	4.17E−07	2.2	Silenced	No	No	No	No	No
	12	4.61E−06	1.7	Silenced	Putative GMC-type oxidoreductase	R135	YP_003986627	Oxidative pathways	MALDI-MS
	13	7.92E−06	1.7	Silenced	Putative GMC-type oxidoreductase	R135	YP_003986627	Oxidative pathways	MALDI-MS
	14	4.04E−05	1.8	Silenced	Putative core protein	L410	YP_003986914	Particle structure	MALDI-MS
	23	1.01E−05	3.1	Silenced	No	No	No	No	No
	24	4.36E−05	2.2	Silenced	Putative BTB/POZ domain-containing protein	L107	YP_00398659	Transcription	MALDI-MS
	25	0.00056	1.6	Silenced	Uncharacterized protein	R553	YP_003987068	Other	MALDI-MS
	28	0.00022	2.7	Silenced	Uncharacterized protein	L442	YP_003986949	ORFan	Nano-LC-MS
	40	0.00041	1.7	Silenced	Putative DNA directed RNA polymerase subunit	R470	YP_003986977	Transcription	Nano-LC-MS
	41	6.74E−05	1.6	Silenced	Capsid protein	L425	YP_003986929	Particle structure	MALDI-MS
	45	0.00086	1.9	Silenced	Uncharacterized protein	R553	YP_003987068	Other	Nano-LC-MS

(Continued on next page)

TABLE 2 (Continued)

Regulation	Spot no.	ANOVA (*P*)	Fold change from wild type/silenced	Highest mean	Protein	Locus tag	Accession no.	Functional category[a]	Identification method
	47	1.45E−05	2.3	Silenced	Uncharacterized protein	L442	YP_003986949	ORFan	Nano-LC-MS
	48	0.00021	1.7	Silenced	Uncharacterized protein	L442	YP_003986949	ORFan	Nano-LC-MS
	50	3.72E−06	1.7	Silenced	Putative alpha/beta hydrolase	R526	YP_003987040	Protein/lipid modification	MALDI-MS
	51	0.00088	1.5	Silenced	Putative alpha/beta hydrolase	R526	YP_003987040	Protein/lipid modification	MALDI-MS
	52	0.00050	2.1	Silenced	Uncharacterized protein	L591	YP_003987106	ORFan	Nano-LC-MS
	55	0.00072	1.8	Silenced	Uncharacterized protein	L725	YP_003987254	ORFan	Nano-LC-MS
	57	0.00017	1.6	Silenced	Uncharacterized protein	L567	YP_003987083	Other	MALDI-MS
	61	0.00111	1.6	Silenced	Probable FAD-linked sulfhydryl oxidase	R596	YP_003987112	Oxidative pathways	MALDI-MS
	62	0.00101	1.8	Silenced	Uncharacterized protein	L724	YP_003987253	ORFan	Nano-LC-MS
	63	0.00084	1.7	Silenced	Uncharacterized protein	R463	YP_003986970	ORFan	MALDI-MS
	64	0.00042	3	Silenced	Uncharacterized protein	L567	YP_003987083	Other	Nano-LC-MS
	65	0.00605	2.3	Silenced	Uncharacterized protein	R463	YP_003986970	ORFan	Nano-LC-MS
	67	0.00068	3.5	Silenced	Uncharacterized protein	R513b	YP_003987026	Other	Nano-LC-MS
	76	0.00018	2.1	Silenced	Uncharacterized protein	R513b	YP_003987026	Other	Nano-LC-MS
	77	0.00064	2	Silenced	Thioredoxin domain-containing protein	R362	YP_003986866	Oxidative pathways	Nano-LC-MS
	83	0.00189	1.5	Silenced	Uncharacterized protein	L442	YP_003986949	ORFan	MALDI-MS

[a]A list of downregulated and upregulated protein spots identified in mimivirus particles is presented. ORF products without a significant database match are denoted as "ORFan." ORF products with significant database matches but with which no functional attribute could be consistently associated through sequence analysis are classified as "Other." No, no identification.

Five proteins (L410, L425, L442, R345, and L725) were found in both downregulated and upregulated isoform spots. These peptide spots were more common in downregulated than upregulated spots, corresponding to 3 spots compared to 1 spot for L410, 12 spots compared to 4 spots for L425, 9 spots compared to 4 spots for L442, and 4 spots compared to 1 spot for L725. In contrast, the abundances of spots for the R345 protein were the same in both downregulated and upregulated spots.

DISCUSSION

In addition to the structural complexity of mimivirus, it also has a large and complex genome (1, 3, 17). The discovery of protein-coding genes belonging to translation in its genome is highly intriguing as their biological importance remains unknown (18, 19). This spectacular discovery was a milestone in virology since, prior to this, no virus was previously known to harbor sequences related to the translational apparatus, reigniting the old debate as to whether viruses are living organisms and whether they deserve a special place in the tree of life. The fact that mimivirus possess genes that encode protein factors involved in translation, along with aa-RSs and tRNAs, contradicted the dogma which had been established by A. Lwoff and colleagues (4, 9, 20–22). This point was further stressed with the description of new *Klosneuvirus* genomes belonging to the new subfamily of *Mimiviridae* which expanded a complement of translation system components, including 25 tRNA, 19 aa-RS, and 40 factor proteins (23). Despite the presence of all these proteins, the fact that they lack ribosomes suggests that they are entirely dependent on the host machinery for protein synthesis.

In this report, we present the first experimental evidence related to a mimivirus translation-related gene, R458, which is predicted to initiate protein biosynthesis. The R458 mimivirus protein is a central component of translation and is absent in other viruses, except *Megavirales*. Its sequence shows a close affinity with different eukaryotic lineages, suggesting that it was acquired from its eukaryotic hosts at different stages of evolution (12). Furthermore, as described here, all R458 domains are well conserved and relate to the wide variety of eukaryotic eIF4a proteins (Fig. 1). According to numerous reports published over the past 20 years, the R458 protein could be involved in several processes, including mRNA binding to the ribosome and unwinding RNA secondary structures in the 5′ untranslated region (UTR) of mRNAs, enabling the efficient binding of the small ribosomal subunit, and subsequent scanning for the initiator codon (14). This resulted in our hypothesis that the mimivirus could possess a putative alternative translation process. We proposed a putative diagram of the regulation of the R458 mimivirus during initiation of translation (Fig. 9). We proposed that

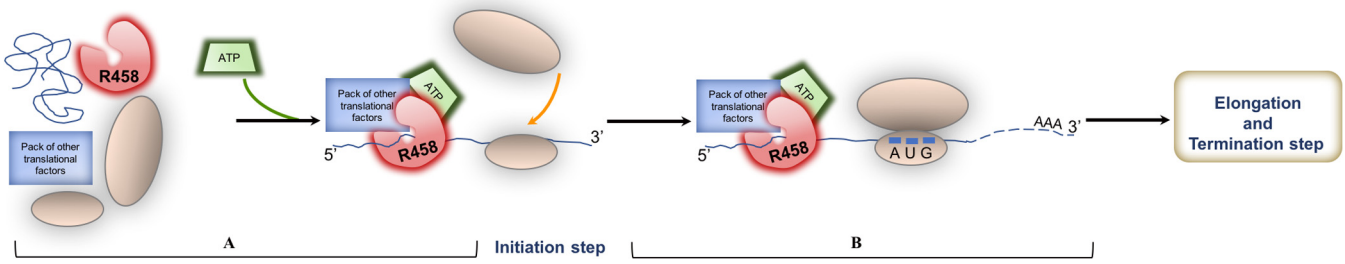

FIG 9 Putative regulation of R458 mimivirus during initiation of translation. (A) Association of R458 with the noncoding RNA initiates the translation by stimulating the ATP activity of R458 and binds with a complex of other translational factors. (B) The small ribosomal subunit initiation complex scans through the 5′ untranslated region for the first AUG initiator codon to begin translation.

the presence of translational genes in the mimivirus genome suggested that these may play a control role in successful replication and correct mRNA translation.

Here, using siRNA, we showed that silencing the R458 gene significantly altered the mRNA mimivirus translation, causing an important deregulation in protein expression (Fig. 8). However, this did not affect the final multiplication of the mimivirus but rather delayed its growth and decreased its fitness. Nevertheless, by studying the development of the mimivirus cycle using fluorescence microscopy and specific polyclonal antibodies, we observed a longer eclipse phase in silenced mimivirus than in wild-type mimivirus and saw that virus factories appeared at least 2 h later. This decline in fitness suggests that the mimivirus requires time to adapt its protein synthesis machinery for transcribing its mRNA when the R458 protein is silenced. Potentially, the delay reflects the time required to compensate for silencing R458 by recruiting functionally equivalent proteins from the amoeba host. In evolutionary terms, the role of R458 might be to enable the earlier formation of virus factories.

We were unable, therefore, to find evidence of a global impact on virus multiplication in the model used in allopatry. However, the translational proteins could be crucial in natural environments when the mimivirus competes with other microorganisms such as virophages, bacteria, archaea, or other viruses multiplying inside amoeba, as demonstrated experimentally in a simple model (24). Alternatively, the translational genes in mimivirus could also play a role in its adaptation to different hosts under different environmental conditions, with metabolic systems which are different from that of *Acanthamoeba*.

Using silencing, a completion of 2D-DIGE gels coupled to MALDI-TOF MS and to nano-LC-MS also identified 81 of the 83 peptide spots. Proteins identified from these gels correlated well to observed and theoretical isoelectric points (pI) and molecular weight (M_w) values. Furthermore, the analysis of 2D-DIGE gels revealed several isoforms and cleaved proteins, a phenomenon found in many viruses and due, in part, to posttranslational modification (phosphorylation, glycosylation, alkylation, acetylation, maturation, and proteolysis) (25–27). However, the possibility of partial degradation of our samples due to contaminating proteases cannot be formally excluded, despite the reproducibility of our gel profiles. It is noteworthy that no amoeba proteins were identified in our samples, confirming mimivirus purity.

In this study, comparative proteomics indicated deregulation in the expression of 32 proteins, 20 of which were identified as downregulated and 17 of which were identified as upregulated. Five of these proteins were detected in both upregulated and downregulated spot isoforms, suggesting a deregulation of posttranslational modification proteins and/or processing (PTMs). Moreover, most of the identified mimivirus spots represented ORFans or had unknown functions. The rest were implicated in the structure of viral particles, oxidative pathways, transcription, modification of proteins and lipids, and DNA topology and repair. According to previous studies (4), most of these deregulated genes are transcribed 6 h postinfection. Only four of them, encoding proteins implicated in transcription (L107 and R470) and particle structure (L410) and of unknown function (L823), are transcribed early (between 0 and 3 h postinfection).

TABLE 3 siRNA used in this study

Target gene	Sequence (DNA)	Primer orientation	Primer sequence (duplex)	%GC
siRNA-R458	GCACTAGTTGTTCCGGAAT	Sense Antisense	GCACUAGUUGUUCCGGAAU AUUCCGGAACAACUAGUGC	47.37

Therefore, considering the fact that R458 is a functional protein, we speculate that translation of mimivirus mRNA may first rely on the amoeba translational machinery only and that the mimivirus then in part uses its own translational machinery and amino acid usage to complete protein synthesis (19). The fact that most deregulated proteins are encoded by late translated genes is in line with this suggestion.

The discovery of viral translational molecules blurs the sharp division between viruses and cellular life (28). This finding emphasizes the dynamic evolution of giant viruses, under the hypothesis that their origins and abundances are determined by the host lifestyle and the pathogens with which they are in competition inside cells (24). In conclusion, translation initiation is the rate-limiting step of protein biosynthesis and is tightly regulated. Here, our data showed that this R458 translation-related factor encoded by the mimivirus is functional during at least part of the infection cycle. The presence of factors belonging to the initial step of translation in the mimivirus suggests that this virus has a weaker dependence on its host, at least in late phases of its replication cycle, than classical viruses.

MATERIALS AND METHODS

Mimivirus and cell preparation. The *Acanthamoeba polyphaga* Link-AP1 trophozoite strain was cultured in peptone-yeast extract-glucose (PYG) medium at 32°C for 3 days as described previously (29). Briefly, *A. polyphaga* protozoa were suspended three times in Page's modified Neff's amoeba saline (PAS) to obtain 5×10^5 cells/ml. Mimivirus was produced in coculture with fresh *A. polyphaga* in PYG medium and purified using low-speed centrifugation ($700 \times g$/10 min). The supernatant was filtered through a 0.8-μm-pore-size filter to remove residual amoebas and cysts. The supernatant was then washed three times in PAS by high-speed centrifugation ($10{,}300 \times g$/10 min) to pellet the viruses. The pellets were then resuspended in 25% sucrose and centrifuged at $10{,}300 \times g$ for 10 min.

siRNA transfection. We targeted the mimivirus R458 gene using short interfering RNA (siRNA) silencing. In order to control the specificity of siRNA for the R458 gene, we performed BLASTn searches against mimivirus and *Acanthamoeba* genes. A fluorescent oligonucleotide primer system (Invitrogen RNA silencing duplex [siRNA]) was designed and purchased from the Invitrogen website (Table 3). One hour before transfection, 10 ml of rinsed 5×10^5cells/ml of *A. polyphaga* was put on the plate to adhere. We then diluted a 20 μM solution of duplex siRNA and 100 μl of Lipofectamine RNAiMAX (Invitrogen) in 400 μl of PAS according to the manufacturer's recommendations. To improve siRNA specificity, we used duplex siRNA and checked for specific and nonspecific pairing. Following siRNA-Lipofectamine suspension, 10^6 mimivirus particles were added to the plate containing the amoeba to achieve a multiplicity of infection (MOI) of 0.2 mimivirus/amoeba. After 1 h of incubation at 32°C, the supernatant was gently removed to eliminate the mimivirus particles and siRNA that were not internalized by the amoebas, and the pellet was resuspended in 10 ml of fresh PAS. This time point was defined as H0. The coculture was then incubated for 24 h at 32°C. Wild-type mimivirus was inoculated, as described above, under the same conditions with the same concentration of mimivirus particles and the same concentration of Lipofectamine reagent as were used for the silenced mimivirus.

To control siRNA transfection inside amoeba, a DMI6000 (Leica DMI 6000B) fluorescence microscope was used to visualize the green fluorescence of the oligonucleotides that were transfected into the amoeba.

Reverse transcription-PCR (RT-PCR). Six hours posttransfection, infected amoeba cells were harvested for RT-PCR analysis using an RNeasy minikit (Qiagen, Crawley, United Kingdom) according to the manufacturer's instructions and recommendations. The mimivirus total RNA was reverse transcribed to cDNA using a SuperScript Vilo cDNA synthesis kit (Invitrogen) according to the manufacturer's instructions. The RT-PCR was performed in an automated PTC-200 thermal cycler (MJ Research) as follows: 25°C for 10 min, 42°C for 60 min, and 85°C for 5 min. Primers for PCR amplification were designed using PrimerQuest (Table 4). These were used to amplify the cDNA of R458. Primers were designed to give an amplicon of approximately 671 bp. Primer sequences were screened using a BLAST search to confirm their specificity. PCR was performed with an automated PTC-200 thermal cycler (MJ Research) in a final volume of 25 μl of PCR mixture, and the PCR products were run on an agarose gel to confirm that products of the expected size were detected.

Fitness comparison between wild-type and silenced mimivirus. After 0, 8, 16, and 24 h postinfection, 200 μl of coculture was used for DNA extraction and quantitative PCRs (qPCRs) to evaluate mimivirus multiplication. DNA extraction was performed using an EZ1 DNA tissue kit (Qiagen, Hilden, Germany) according to the manufacturer's instructions. The qPCRs were performed in a CFX96 thermal

TABLE 4 Primers for R458 gene amplification

Organism primer	ORF	Sequence (5′–3′)	Position	Expected amplicon size (bp)
Mimivirus-F Mimivirus-R	R458	GATGGTGCAACTTCAACAGTTT TCAGCCATCTGATCTTCAGTATTC	210 to 881	671

cycler (Bio-Rad Laboratories, Foster City, CA, USA) using Syber green PCR master mix (Qiagen) according to the manufacturer's instructions to quantify the replication of mimivirus DNA.

Quantification of mimivirus particles was achieved using an endpoint dilution assay to evaluate mimivirus infectious particles at each time point (H0, H8, H16, and H24).

Other amoebas were infected with silenced mimivirus collected at 24 h postinfection, and propagation of the second-generation mimivirus then followed using qPCRs to evaluate their multiplication.

For immunofluorescence, siRNA against R458 without fluorescence and mimivirus-specific polyclonal anti-mimivirus antibodies which were previously raised in mouse against mimivirus were used. Every 30 min during 24 h, 100 μl cells was spotted on microscope slides using a Cytospin instrument. The indirect immunodetection technique was performed using mouse anti-mimivirus serum, while the remaining cells were stained with Evans Blue dye to highlight the time point when mimivirus factories appeared (1).

Between H2 and H12 postinfection, 1,000 cells were randomly selected and mimivirus factories were quantified. A DMI6000 fluorescence microscope (Leica DMI 6000B) was used to visualize the green fluorescence of the mimivirus antibody in the amoeba.

2D-DIGE analysis and protein MALDI-TOF MS identification. Proteomic analysis was performed by the use of 2D-DIGE as previously described (30). Briefly, four sets of mimivirus virions (obtained 24 h after silencing) from each wild-type and silenced mimivirus were prepared for minimal labeling with Cy dyes. Samples from each group were randomly labeled with cyanine dyes (Cy3 or Cy5) in a ratio of 400 pmol CyDye to 50 μg of proteins. An internal standard was created by combining equal amounts of proteins from every sample, labeled with Cy2 using the same ratio. The sample was labeled for 30 min on ice in the dark, and the reaction was quenched by adding 10 mM lysine according to the instructions of the manufacturer (GE Healthcare). Cy dye-labeled samples were combined during 2D gel electrophoresis processes so that each gel contained Cy2-, Cy3-, and Cy5-labeled proteins. 2D gel electrophoresis was carried out as previously described (31). Following electrophoresis, gels were scanned at the appropriate wavelengths using a Typhoon Trio Imager according to the protocol of the manufacturer (GE Healthcare). Scans were acquired at 100-μm resolution. Images were cropped using ImageQuant software (GE Healthcare) and further analyzed using Progenesis SameSpots software (version 4.0.3779) from Nonlinear Dynamics as described by the manufacturer. To determine significant differences in 2D spot abundance, an analysis of variance (ANOVA) score (*P* value) lower than or close to 0.05 and a fold change value of at least 1.5 for comparisons between mimivirus protein spots were required for spots to be selected for digestion and identification by matrix-assisted laser desorption ionization–time of flight mass spectrometry (MALDI-TOF MS) (Bruker Daltonik, France) as previously described (32).

The gels were subjected to silver staining (33), and differentially regulated spots were excised by transmission scanning (ImageScanner; Amersham) and digested with trypsin (sequencing-grade modified porcine trypsin; Promega, Madison, WI) followed by MALDI-TOF MS identification. Mass analyses were performed on a Brüker Ultraflex spectrometer (Brüker France, Wissembourg, France). Tryptic peptide mass lists were used to identify the proteins by the use of Mascot software and were then compared to the mimivirus protein sequence database (Uniprot; July 2014; 979 sequences) with the following parameters: 90 ppm tolerance; one missed cleavage; carbamidomethyl, C; oxidation, M.

Nano-LC mass spectrometry. Unidentified gel spots digests in MALDI-TOF were analyzed using a nano-LC system coupled with a high-resolution quadrupole-time of flight (Q-TOF) mass spectrometer (nanoAcquity, Synapt G2 Si; Waters, Guyancourt, France). Peptide digests (2 μl) were trapped using a nanoAcquity UPLC Symmetry C_{18} column (180 μm by 20 mm) at 20 μl/min in water–0.1% formic acid and then eluted on an analytical nanoAcquity UPLC HSS T3 column (Waters, Guyancourt, France) (1.8-μm pore size; 75 μm by 250 mm) using a 90-min gradient (5% to 40% acetonitrile–0.1% formic acid–water). Mass spectrometry experiments were performed in positive-ion mode and in resolution mode. The mass range was between 50 and 2,000 *m/z*. The ion source parameters were as follows: capillary voltage, 3 kV; sampling cone voltage, 40 V; ion source temperature, 90°C; cone gas flow, 50 liters/h. The transfer collision low-energy value was set to 5 V, and trap collision low-energy value was set to 4 V. A Lockmass correction was applied using GFP ([Glu1]-fibrinopeptide B) as follows: [M + 2H]2 + 785.8426 *m/z*. Data were processed using ProteinLynx Global Server version 3.0.2 (PLGS; Waters). Processing parameters were 250 counts for the low-energy threshold, 100 counts for the elevated-energy threshold, and 750 counts for the intensity threshold. The database combined the sequences of DNA viruses (27 August 2015; Swiss-Prot and TrEMBL; 424,847 sequences). Up to one missed cleavage was allowed for trypsin. Fixed carbamidomethyl and variable oxidation (M) and carbamylation (K and N terminus [N-term]) were set as modifications.

Accession number(s). GenBank accession numbers for data determined in this work are listed in Table 2.

ACKNOWLEDGMENTS

This work was supported by the French Government under the Investissements d'avenir (Investments for the Future) program managed by the Agence Nationale de la

Recherche (ANR [National Agency for Research]) (reference: Méditerranée Infection 10-IAHU-03).

REFERENCES

1. La Scola B, Audic S, Robert C, Jungang L, de Lamballerie X, Drancourt M, Birtles R, Claverie JM, Raoult D. 2003. A giant virus in amoebae. Science 299:2033. https://doi.org/10.1126/science.1081867.
2. Aherfi S, Colson P, La Scola B, Raoult D. 2016. Giant viruses of amoebas: an update. Front Microbiol 7:349. https://doi.org/10.3389/fmicb.2016.00349.
3. Raoult D, Audic S, Robert C, Abergel C, Renesto P, Ogata H, La Scola B, Suzan M, Claverie JM. 2004. The 1.2-megabase genome sequence of mimivirus. Science 306:1344–1350. https://doi.org/10.1126/science.1101485.
4. Legendre M, Santini S, Rico A, Abergel C, Claverie JM. 2011. Breaking the 1000-gene barrier for mimivirus using ultra-deep genome and transcriptome sequencing. Virol J 8:99. https://doi.org/10.1186/1743-422X-8-99.
5. Forterre P. 2010. Giant viruses: conflicts in revisiting the virus concept. Intervirology 53:362–378. https://doi.org/10.1159/000312921.
6. Colson P, La Scola B, Levasseur A, Caetano-Anollés G, Raoult D. 2017. Mimivirus: leading the way in the discovery of giant viruses of amoebae. Nat Rev Microbiol 15:243–254. https://doi.org/10.1038/nrmicro.2016.197.
7. Abrahão JS, Araújo R, Colson P, La Scola B. 2017. The analysis of translation-related gene set boosts debates around origin and evolution of mimiviruses. PLoS Genet 13:e1006532. https://doi.org/10.1371/journal.pgen.1006532.
8. Abergel C, Rudinger-Thirion J, Giege R, Claverie JM. 2007. Virus-encoded aminoacyl-tRNA synthetases: structural and functional characterization of mimivirus TyrRS and MetRS. J Virol 81:12406–12417. https://doi.org/10.1128/JVI.01107-07.
9. Claverie JM, Abergel C. 2010. Mimivirus: the emerging paradox of quasi-autonomous viruses. Trends Genet 26:431–437. https://doi.org/10.1016/j.tig.2010.07.003.
10. Legendre M, Audic S, Poirot O, Hingamp P, Seltzer V, Byrne D, Lartigue A, Lescot M, Bernadac A, Poulain J, Abergel C, Claverie JM. 2010. mRNA deep sequencing reveals 75 new genes and a complex transcriptional landscape in mimivirus. Genome Res 20:664–674. https://doi.org/10.1101/gr.102582.109.
11. Sobhy H, La Scola B, Pagnier I, Raoult D, Colson P. 2015. Identification of giant mimivirus protein functions using RNA interference. Front Microbiol 6:345. https://doi.org/10.3389/fmicb.2015.00345.
12. Yutin N, Wolf YI, Koonin EV. 2014. Origin of giant viruses from smaller DNA viruses not from a fourth domain of cellular life. Virology 466–467:38–52. https://doi.org/10.1016/j.virol.2014.06.032.
13. Lin D, Pestova TV, Hellen CU, Tiedge H. 2008. Translational control by a small RNA: dendritic BC1 RNA targets the eukaryotic initiation factor 4A helicase mechanism. Mol Cell Biol 28:3008–3019. https://doi.org/10.1128/MCB.01800-07.
14. Andreou AZ, Klostermeier D. 2013. The DEAD-box helicase eIF4A: paradigm or the odd one out? RNA Biol 10:19–32. https://doi.org/10.4161/rna.21966.
15. Newman JA, Savitsky P, Allerston CK, Bizard AH, Özer Ö, Sarlós K, Liu Y, Pardon E, Steyaert J, Hickson ID, Gileadi O. 2015. Crystal structure of the Bloom's syndrome helicase indicates a role for the HRDC domain in conformational changes. Nucleic Acids Res 43:5221–5235. https://doi.org/10.1093/nar/gkv373.
16. Azza S, Cambillau C, Raoult D, Suzan-Monti M. 2009. Revised mimivirus major capsid protein sequence reveals intron-containing gene structure and extra domain. BMC Mol Biol 10:39. https://doi.org/10.1186/1471-2199-10-39.
17. Moreira D, Brochier-Armanet C. 2008. Giant viruses, giant chimeras: the multiple evolutionary histories of mimivirus genes. BMC Evol Biol 8:12. https://doi.org/10.1186/1471-2148-8-12.
18. Jeudy S, Abergel C, Claverie JM, Legendre M. 2012. Translation in giant viruses: a unique mixture of bacterial and eukaryotic termination schemes. PLoS Genet 8:e1003122. https://doi.org/10.1371/journal.pgen.1003122.
19. Colson P, Fournous G, Diene SM, Raoult D. 2013. Codon usage, amino acid usage, transfer RNA and amino-acyl-tRNA synthetases in mimiviruses. Intervirology 56:364–375. https://doi.org/10.1159/000354557.
20. Lwoff A. 1957. The concept of virus. J Gen Microbiol 17:239–253.
21. Lwoff A, Tournier P. 1966. The classification of viruses. Annu Rev Microbiol 20:45–74. https://doi.org/10.1146/annurev.mi.20.100166.000401.
22. Claverie JM, Ogata H, Audic S, Abergel C, Suhre K, Fournier PE. 2006. Mimivirus and the emerging concept of "giant" virus. Virus Res 117:133–144. https://doi.org/10.1016/j.virusres.2006.01.008.
23. Schulz F, Yutin N, Ivanova NN, Ortega DR, Lee TK, Vierheilig J, Daims H, Horn M, Wagner M, Jensen GJ, Kyrpides NC, Koonin EV, Woyke T. 2017. Giant viruses with an expanded complement of translation system components. Science 356:82–85. https://doi.org/10.1126/science.aal4657.
24. Slimani M, Pagnier I, Raoult D, La Scola B. 2013. Amoebae as battlefields for bacteria, giant viruses, and virophages. J Virol 87:4783–4785. https://doi.org/10.1128/JVI.02948-12.
25. Vanslyke JK, Whitehead SS, Wilson EM, Hruby DE. 1991. The multistep proteolytic maturation pathway utilized by vaccinia virus P4a protein: a degenerate conserved cleavage motif within core proteins. Virology 183:467–478. https://doi.org/10.1016/0042-6822(91)90976-I.
26. Johnson JE. 1996. Functional implications of protein-protein interactions in icosahedral viruses. Proc Natl Acad Sci U S A 93:27–33.
27. Moulard M, Decroly E. 2000. Maturation of HIV envelope glycoprotein precursors by cellular endoproteases. Biochim Biophys Acta 1469:121–132. https://doi.org/10.1016/S0304-4157(00)00014-9.
28. Nasir A, Caetano-Anollés G. 2015. A phylogenomic era data-driven exploration of viral origins and evolution. Sci Adv 1:e1500527. https://doi.org/10.1126/sciadv.1500527.
29. Mba Medie F, Ben-Salah I, Henrissat B, Raoult D, Drancourt M. 2011. *Mycobacterium tuberculosis* complex mycobacteria as amoeba-resistant organisms. PLoS One 6:e20499. https://doi.org/10.1371/journal.pone.0020499.
30. Boyer M, Azza S, Barrassi L, Klose T, Campocasso A, Pagnier I, Fournous G, Borg A, Robert C, Zhang X, Desnues C, Henrissat B, Rossmann MG, La Scola B, Raoult D. 2011. Mimivirus shows dramatic genome reduction after intraamoebal culture. Proc Natl Acad Sci U S A 108:10296–10301. https://doi.org/10.1073/pnas.1101118108.
31. Renesto P, Abergel C, Decloquement P, Moinier D, Azza S, Ogata H, Fourquet P, Gorvel JP, Claverie JM. 2006. Mimivirus giant particles incorporate a large fraction of anonymous and unique gene products. J Virol 80:11678–11685. https://doi.org/10.1128/JVI.00940-06.
32. Suhre K. 2005. Gene and genome duplication in *Acanthamoeba polyphaga* mimivirus. J Virol 79:14095–14101. https://doi.org/10.1128/JVI.79.22.14095-14101.2005.
33. Shevchenko A, Wilm M, Vorm O, Mann M. 1996. Mass spectrometric sequencing of proteins silver-stained polyacrylamide gels. Anal Chem 68:850–858. https://doi.org/10.1021/ac950914h.